Available online at www.sciencedirect.com
SCIENCE DIRECT®
International Journal of Thermal Sciences 45 (2006) 932–937
International Journal of Thermal Sciences
www.elsevier.com/locate/ijts

Developing upward flow in a uniformly heated circular duct under transitional mixed convection

Walter Grassi *, Daniele Testi

LOTHAR (LOw gravity and THermal Advanced Research Laboratory), Department of Energetics "L. Poggi", University of Pisa, via Diotisalvi 2, 56126 Pisa, Italy

Received 16 September 2005; received in revised form 31 October 2005; accepted 17 November 2005

Available online 19 January 2006

Abstract

Upward flow of perfluorohexane (*FC-72*) in the entry zone of a uniformly heated circular duct was studied in a regime of transitional combined forced and free convection. Heat transfer coefficients were measured along the heated length at different values of flow rate and heat flux. Heat transfer impairment in the developing region due to laminarisation of the turbulent flow was observed and characterised by means of two well-known dimensionless groups: the Grätz number and the Grashof number based on the wall heat flux.

Keywords: Mixed convection; Developing flow; Buoyancy; Entrance region; Heat transfer correlations; Laminarisation

1. Introduction

In a weakly forced pipe flow, the buoyant forces can be of the same order of magnitude as the inertial ones. In this condition of mixed convection, the hydrodynamic and the thermal fields are interdependent. The velocity and temperature profiles of the pure forced convection case are modified by buoyancy; moreover, turbulence arises much earlier: at $Re \approx 400$ for vertical tubes and $Re \approx 1000$ for horizontal ones, according to the maps proposed in [1].

The internal heat transfer characteristics in mixed convection not only depend on whether the flow is hydrodynamically or thermally developing, laminar or turbulent and on duct geometry, but also on whether the fluid is cooled or heated and on duct orientation (horizontal or inclined, upflow or downflow).

1.1. Vertical aiding flow

In the vertical aiding configuration (heated upflow or cooled downflow) laminarisation effects may be observed. The description of the phenomenon is the following: when natural and forced convection act in the same direction, the fluid is accelerated in the region close to the tube wall and, due to mass continuity, retarded in the core (see Fig. 1).

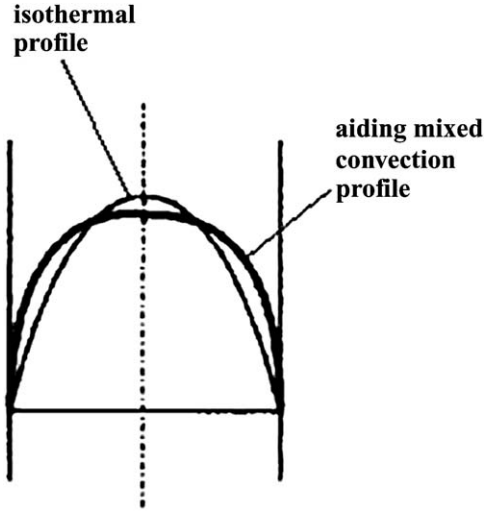

Fig. 1. Velocity profiles under isothermal and aiding flow [2].

According to Prandtl's model of turbulence, heat transfer is mainly controlled by the diffusive energy transport from the border of the viscous layer (in which the transfer is conduc-

* Corresponding author. Tels: +39 050 2217090, +39 050 2217109; fax: +39 050 2217085.

E-mail addresses: w.grassi@ing.unipi.it (W. Grassi), d.testi@ing.unipi.it (D. Testi).

1290-0729/$ – see front matter
doi:10.1016/j.ijthermalsci.2005.11.007

Nomenclature

c_p	fluid specific heat	$\mathrm{J\,kg^{-1}\,K^{-1}}$	
D	duct inner diameter	m	
g	acceleration due to gravity	$\mathrm{m\,s^{-2}}$	
Gr	$=\frac{\beta g(T_{w\_\mathrm{in}}-T_b)D^3}{\nu^2}$, Grashof number based on the wall superheat		
Gr_q	Grashof number based on the wall heat flux		
Gz	Grätz number		
L	duct heated length	m	
$\dot{m}$	$=\rho\dot{V}$, mass flow rate	$\mathrm{kg\,s^{-1}}$	
Nu	Nusselt number		
$\langle Nu\rangle$	azimuthal average of the Nusselt number		
Pr	Prandtl number		
q	wall heat flux	$\mathrm{W\,m^{-2}}$	
Re	Reynolds number		
s	duct thickness	m	
T	temperature	K	
u	fluid velocity	$\mathrm{m\,s^{-1}}$	
u_m	mean velocity in the core of the flow	$\mathrm{m\,s^{-1}}$	
u_ε	velocity at the rim of the viscous layer	$\mathrm{m\,s^{-1}}$	
$\dot{V}$	volumetric flow rate	$\mathrm{m^3\,s^{-1}}$	
x	distance from the thermal inlet section	m	
x^*	$=Gz^{-1}$, normalised distance from the inlet		

Greek symbols

α	convective heat transfer coefficient	$\mathrm{W\,m^{-2}\,K^{-1}}$
β	coefficient of cubic expansion	$\mathrm{K^{-1}}$
η	dynamic viscosity	Pa s
λ	fluid thermal conductivity	$\mathrm{W\,m^{-1}\,K^{-1}}$
ν	$=\frac{\eta}{\rho}$, kinematic viscosity	$\mathrm{m^2\,s^{-1}}$
Θ	heat flow	W
ρ	mass density	$\mathrm{kg\,m^{-3}}$

Subscripts

b	bulk
f	film
i	insulator
in	inlet
out	outlet
w	wall
w_in	inner side of the heated wall
w_out	outer side of the heated wall

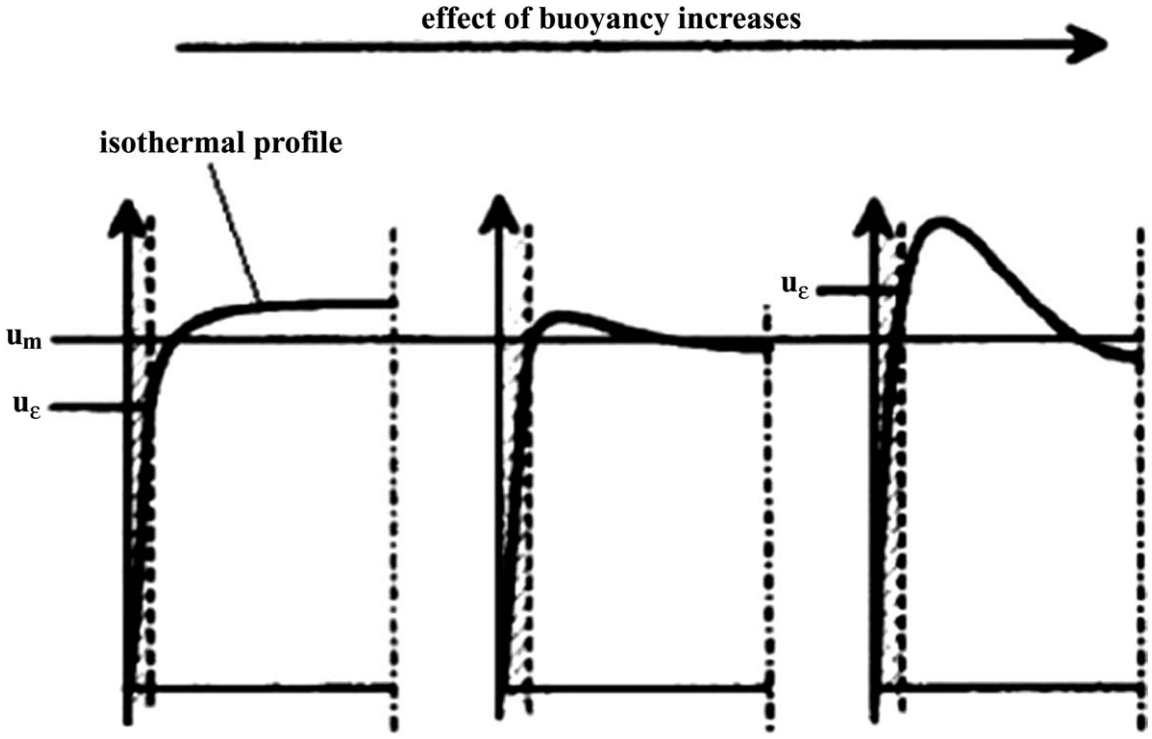

Fig. 2. Effect of buoyancy level on the velocity profile [2].

tive) to the core of the turbulent flow. The mentioned energy transport increases in accordance with the production of turbulence in the area close to the edge of the viscous layer, which, in turn, depends on the difference between the mean velocity in the core of the flow, u_m, and the velocity at the rim of the viscous layer, u_ε (see Fig. 2).

In the middle drawing of Fig. 2, the difference between u_m and u_ε is close to zero, thus, the reduced turbulence production causes a laminarisation of the flow and a consequent heat transfer impairment. In a thermally developing flow, this phenomenon is likely to occur at a certain distance from the inlet, depending on the imposed flow rate and heat flux [3].

Table 1
FC-72 physical properties at 25 °C and 1 bar

Freezing point	−90 °C
Boiling point	56 °C
Density	1.68×10^3 kg m^{-3}
Kinematic viscosity	3.8×10^{-7} m^2 s^{-1}
Specific heat	1.1×10^3 J kg^{-1} K^{-1}
Thermal conductivity	5.7×10^{-2} W m^{-1} K^{-1}
Coefficient of expansion	1.56×10^{-3} K^{-1}

Although a comprehensive account of turbulent mixed convection can be found in [4], fundamental understanding of the heat transfer behaviour of combined free and forced convection in the thermal entry region is very limited, in spite of the fact that in practical applications we rarely deal with a fully developed flow.

2. Experimental apparatus

In the present work we analyse the developing regime of mixed convection in a circular pipe positioned vertically, with upward flow.

2.1. Working fluid

The fluid chosen for the experimental campaign is perfluorohexane, a Fluorinert™ Electronic Liquid manufactured by *3M* (St. Paul, MN, USA), commercially named *FC-72*. The main physical properties of this dielectric liquid are reported in Table 1.

FC-72 is thermally and chemically stable, compatible with sensitive materials, non-flammable, non-toxic, colourless, and has no ozone depletion potential. This combination of properties, together with its particularly low viscosity, makes *FC-72* appropriate for applications like heat sinks for electronic components.

2.2. Test loop description

A test loop was built as shown in the schematic of Fig. 3.

The fluid, moved by a gear pump, circulated through the test specimen at volumetric flow rates in the range 0.26–1.04 lt min^{-1}. A flowmeter measured the flow rate with an accuracy of ±0.0086 lt min^{-1}. The fluid, uniformly heated in its flow along the test section, was cooled to the desired inlet temperature by means of a shell-tube heat exchanger, with countercurrent chilled water flowing in the shell. An expansion vessel was used to compensate the volume increase in the loop due to temperature variations and to set the pressure of the position it was mounted on. An absolute pressure transducer was placed right upstream of the gear pump, in order to check that the lowest pressure of the loop was above the room pressure, thus avoiding air from being sucked in by the pump. All the tests were performed at an inlet temperature of 20 °C and at an absolute pressure of 2 bars.

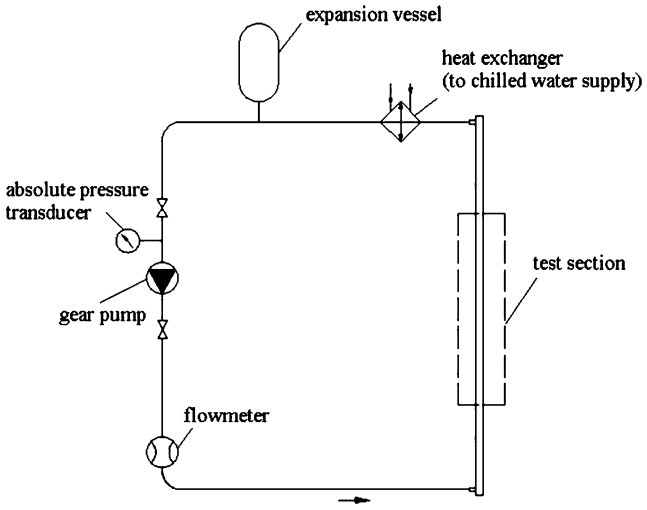

Fig. 3. Schematic of the test loop.

2.3. Test section description

A detailed schematic of the test section is shown in Fig. 4.

The pipe was made of stainless steel and had an inner diameter $D = 17.3$ mm and a wall thickness $s = 2$ mm. After an abrupt contraction, a short unheated length (about 7 diameters long) precedes the thermal entrance. The fluid was warmed up by an electrical resistance heater applied to the outer wall for a length $L = 500$ mm. The applied heat flow ranged from 30 to 85 W.

Temperature measurements were made by type-T thermocouples, placed on the outer wall, under the heater, at three cross sections along the heated length: respectively at $x = 125$ mm, $x = 250$ mm, and $x = 375$ mm, being x the distance from the beginning of the heated length. Each cross section had four thermocouples, one every 90°.

To minimize heat losses, the entire specimen was covered with a thermal insulator ($\lambda_i = 0.038$ W m^{-1} K^{-1}). Two more type-T thermocouples were placed at the inlet and at the outlet of the test section, in order to evaluate the heat flow supplied in steady state through the energy balance:

$$\Theta = \dot{m} c_p (T_{\text{out}} - T_{\text{in}}) \tag{1}$$

having neglected the heat generated by viscous dissipation within the fluid.

All the thermocouples used a zero-point reference joint, whose temperature was controlled by a reference resistance thermometer. The overall accuracy of each thermocouple after calibration in the 15–60 °C range was ±0.2 K.

The available differential pressure transducer had a sensitivity of 30 Pa and was not able to measure appreciable pressure drops through the test section.

Further details on the experimental apparatus can be found in [5].

3. Test procedure and data analysis

Every test was run under constant volumetric flow rate and heat flow and a steady state condition was awaited. The ther-

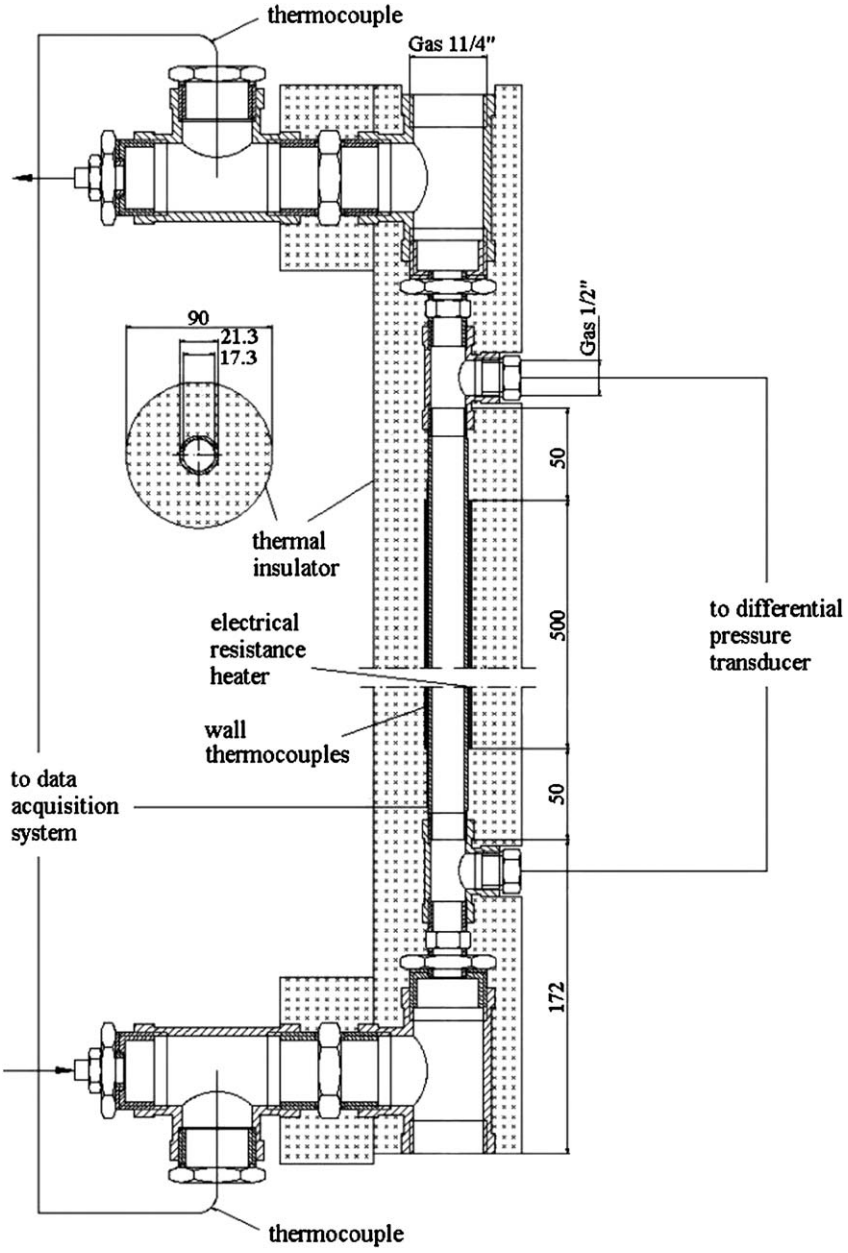

Fig. 4. Detail of the test section.

mocouples' signals were acquired every 6 seconds by a scanner mounted on a digital multimeter; then the data were sent to a PC in order to be recorded and processed.

The bulk temperature of the fluid at a given axial position was calculated considering a temperature of adiabatic mixing for the examined cross section, assuming a linear trend, from the inlet to the outlet temperature, on the heated length. The temperatures of the inner side of the wall were obtained from the ones measured on the outer face, properly accounting for one-dimensional heat conduction within the duct thickness:

$$T_{w\_\mathrm{in}} = T_{w\_\mathrm{out}} - \frac{\Theta}{2\pi\lambda_w L}\ln\left(\frac{D+2s}{D}\right) \tag{2}$$

The dimensionless numbers describing mixed convection in uniform heat flux conditions (i.e.: Nu, Re, Gr_q, and Pr) were calculated as:

$$Nu = \frac{\alpha D}{\lambda_f} = \frac{qD}{\lambda_f(T_{w\_\mathrm{in}} - T_b)} = \frac{1}{\pi}\frac{\Theta}{\lambda_f(T_{w\_\mathrm{in}} - T_b)L} \tag{3}$$

$$Re = \frac{u\rho_{\mathrm{in}}D}{\eta_{\mathrm{in}}} = \frac{4}{\pi}\frac{\dot{V}}{D\nu_{\mathrm{in}}} \tag{4}$$

$$Gr_q = GrNu = \frac{\beta_{\mathrm{in}}gqD^4}{\lambda_{\mathrm{in}}\nu_{\mathrm{in}}^2} = \frac{1}{\pi}\frac{\beta_{\mathrm{in}}g\Theta D^3}{\lambda_{\mathrm{in}}\nu_{\mathrm{in}}^2 L} \tag{5}$$

$$Pr = \frac{\eta_{\mathrm{in}}c_p}{\lambda_{\mathrm{in}}} \tag{6}$$

having defined the film temperature as:

$$T_f = \frac{T_b + T_{w\_\mathrm{in}}}{2} \tag{7}$$

Even at the highest heat flow, the temperatures of the fluid in correspondence of the inner side of the heated wall (T_{w_in}) were fairly below the boiling point, never exceeding 50 °C.

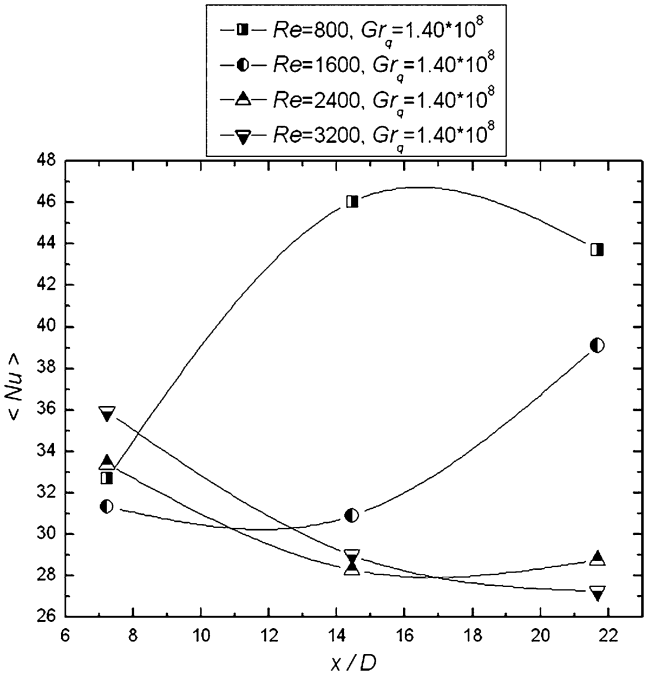

Fig. 5. $\langle Nu \rangle$ vs. x/D at a fixed Gr_q and fourdifferent Re.

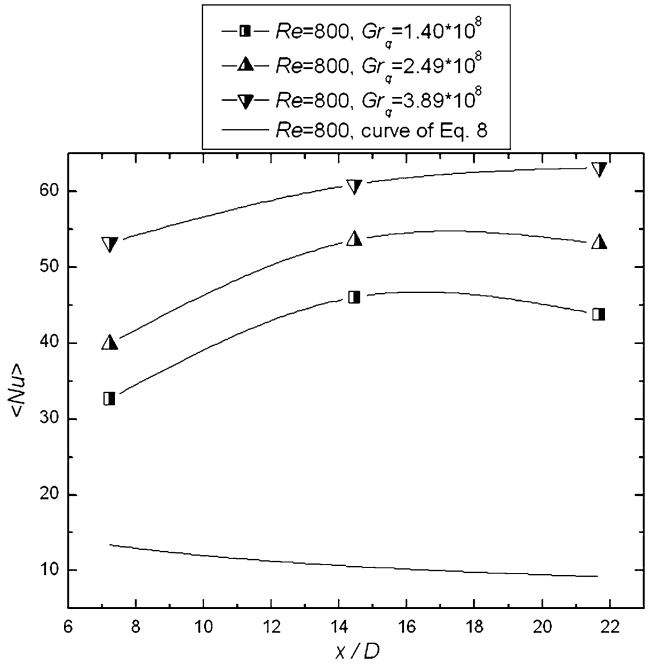

Fig. 6. $\langle Nu \rangle$ vs. x/D at a fixed Re and three different Gr_q, compared with the curve of Eq. (8).

The maximum experimental error on the Nusselt number, corresponding to the lowest temperature difference between T_{w_in} and T_b, was 2.7%, while the maximum relative error on the Reynolds number, obtained at the lowest flow rate, was 3.6%.

4. Discussion of heat transfer results

In every test, the data were obtained averaging 50 measurements recorded consecutively once a steady state condition was reached. The Grashof number based on the wall heat flux ranged from 1.40×10^8 to 3.89×10^8, while the Reynolds number from 800 to 3200. Having worked with a single fluid, the Prandtl number, as defined by Eq. (6), did not vary and was equal to 11.9.

The Nusselt number results are presented as an azimuthal average, $\langle Nu \rangle$, made on the four thermocouples present at each of the three monitored cross sections of the duct.

4.1. Tests at a fixed Gr_q

In the experiments, the flow, even if presumably disturbed, should still be laminar at the thermal inlet section (eventually, transitional at $Re = 3200$).

Observing the results obtained at a fixed heat flux and different flow rates, we can clearly locate a zone of the duct undergoing heat transfer impairment, which moves downstream with increasing Re. This trend is illustrated in Fig. 5 for a heat flow of 30 W and is in accordance with the model of turbulent flow laminarisation described in the introduction section. In fact, at a higher flow rate, more tube length is needed for buoyancy to deform the velocity profile in the duct, up to the critical point of minimum turbulence production.

Besides, since the onset of buoyancy effects is progressively retarded for increasing Reynolds number, the thermal-entrance effect prevails in the initial region for $Re = 2400$ and $Re = 3200$, with consequently higher heat transfer rates.

4.2. Tests at a fixed Re

On the other hand, if we increase the heat flow while keeping a fixed flow rate, we observe a negligible upstream shift of the heat transfer impairment zone. However, at higher Gr_q, we obtain noticeably higher $\langle Nu \rangle$ at every monitored cross section (see Fig. 6).

Moreover, the aiding effect of buoyancy is evident by comparing the measurements with the following constant property correlation [6], valid for laminar forced flow in the entrance region and calculated at $Re = 800$ (see again Fig. 6):

$$\langle Nu \rangle = \max \left\| \begin{array}{c} 0.462 Pr^{1/3} \left(\frac{Re}{x/D}\right)^{1/2} \\ \{4.364^3 + 1 + [1.302 \left(\frac{Re\,Pr}{x/D}\right)^{1/3} - 1]^3\}^{1/3} \end{array} \right\| \quad (8)$$

4.3. $\langle Nu \rangle$ as a function of the Grätz number

In order to have a more compact representation of the experimental data, we need to introduce the Grätz number, defined as:

$$Gz = Re\,Pr \frac{D}{x} \quad (9)$$

By observing the curves of Fig. 7, we realise that the minimum $\langle Nu \rangle$, corresponding to the centre of the laminarised zone, is reached in a very narrow interval of Grätz numbers, around the value of 2000 ($x^* = Gz^{-1} \approx 0.0005$).

In other terms, although the region of laminarisation can be actually moved along the duct by varying the flow rate, x^*, in-

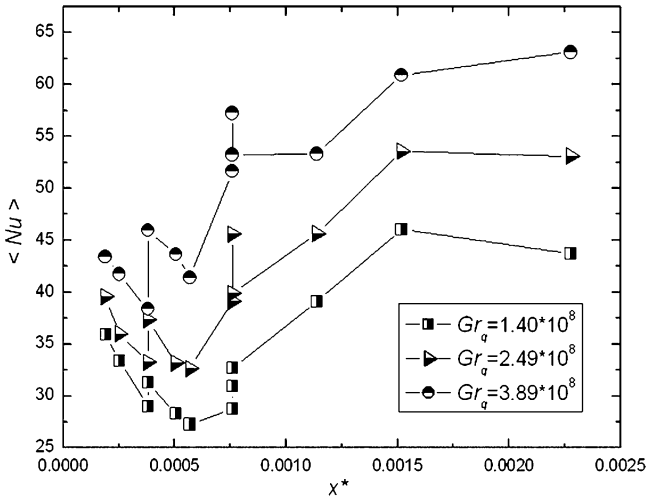

Fig. 7. $\langle Nu \rangle$ vs. x^* at three different Gr_q.

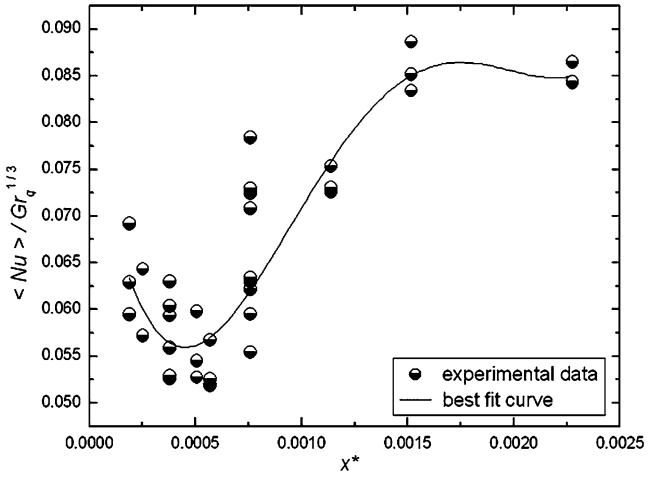

Fig. 8. $\langle Nu \rangle / Gr_q^{1/3}$ vs. x^*.

cluding both x/D and Re in a single parameter, gives a proper normalisation of the distance from the inlet.

However, the experimental setup seems very prone to produce Re-dependent effects in the thermal entrance, because of the presence of unsuppressed fluid-dynamic disturbances, and a partial flow development at $x = 0$. All of this can hardly be integrated in the effect of the Grätz number, but can explain the scattering of the experimental data in Fig. 7.

Finally, plotting $\langle Nu \rangle / Gr_q^{1/3}$ as a function of x^*, we can describe the entire phenomenon, with a reasonable accuracy, by means of a single curve, whose graphical representation is given in Fig. 8. All the experimental data lie within the 20% deviation band, with most of them (83%) within the 10% band.

5. Conclusions

In this work we examined the flow of perfluorohexane in the entry region of a uniformly heated vertical circular pipe in a regime of aiding mixed convection. Under such a complex flow, heat transfer along the tube has a non-monotonic, transitional behaviour, showing a minimum in the laminarised zone. The minimum can be shifted downstream by increasing the Reynolds number; however, in all the tests, it occurs at a Grätz number around 2000. In fact, plotting the Nusselt number versus the Grätz number, the experimental points obtained at different flow rates and at a fixed heat flux seem to lie on a single curve, with a deviation possibly due to entry effects. Increasing the heat flow, this curve simply moves up, to higher heat transfer values. An even more compact representation of the phenomenon can then be obtained by expressing the group $\langle Nu \rangle / Gr_q^{1/3}$ as a function of x^*. In this way, the whole experimental data set is described by a single curve with a reasonable approximation, stressing how the dimensionless numbers Gz and Gr_q should be greatly representative of the studied regime and in particular of the phenomenon of laminarisation.

Acknowledgements

The authors are particularly indebted to Mr. Roberto Manetti for his skillful technical assistance and would also like to thank Dr. Mario Saputelli, who contributed with great commitment to running the experimental apparatus.

References

[1] B. Metais, E.R.G. Eckert, Forced, mixed, and free convection regimes, J. Heat Transfer – Trans. ASME 86 (1964) 295–296.
[2] T. Aicher, H. Martin, New correlations for mixed turbulent natural and forced convection heat transfer in vertical tubes, Int. J. Heat Mass Transfer 40 (15) (1997) 3617–3626.
[3] J.D. Jackson, M.A. Cotton, B.P. Axcell, Studies of mixed convection in vertical tubes, J. Heat Fluid Flow 10 (1) (1989) 2–15.
[4] B.S. Petukhov, A.F. Polyakov, Heat Transfer in Turbulent Mixed Convection, Hemisphere, New York, 1988.
[5] W. Grassi, D. Testi, Heat transfer augmentation by ion injection in an annular duct, J. Heat Transfer – Trans. ASME, in press.
[6] VDI Heat Atlas, VDI-Verlag, Düsseldorf, 1993, Gb 4.